Research Article

BIOMEDICAL Journal of Scientific & Technical Research

ISSN: 2574 -1241

DOI: 10.26717/BJSTR.2022.42.006716

Evaluation of Cell Lysis Due to Ice Crystals in Cell Freezing

Kiyoshi Bando*

Department of Mechanical Engineering, Kansai University, Japan

***Corresponding author:** Kiyoshi Bando, Department of Mechanical Engineering, Kansai University, 3-3-35 Yamate-cho, Suita-city, Osaka 564-8680, Japan

ARTICLE INFO

Received: January 17, 2022

Published: February 28, 2022

Citation: Kiyoshi Bando. Evaluation of Cell Lysis Due to Ice Crystals in Cell Freezing. Biomed J Sci & Tech Res 42(2)-2022. BJSTR. MS.ID.006716.

Keywords: Cell lysis; Cell Freezing; Viability; Compression

ABSTRACT

In cell freezing, when the temperature drop is slow, one of the mechanisms of cell damage is considered to be the development of many needle-like extracellular ice crystals, which narrow the spaces between the needles and compress the cells. The objectives of this study are to derive the membrane tension, the increase in surface area, and the deformation shapes generated in the cells during compression between parallel plates and to investigate the relationship between these factors and the cell viability, as well as the physical mechanism of cell lysis. The cortical actin filaments were modeled as elastic membranes on spherical cells. The intracellular actin filaments, microtubules, and intermediate filaments were approximated as operations to keep the cell volume constant. The tension generated during cell adhesion was expressed as the initial tension of the membrane. Calculations were performed on the prostatic adenocarcinoma cells (PC-3) used in the compression experiment [1]. The results indicated that the expansion tension was the main cause of cell lysis rather than the shear tension. With a larger cell size owing to the effect of external osmotic pressure, more tension was generated in the cells during compression. Therefore, larger cells had lower viability during compression. The surface area of the cells was increased by compression, but the rate of surface area increase was independent of the cell size. The deformation shape of the cells due to compression was also independent of the cell size. Therefore, the surface area increase rate and the deformation shape of the cells were the evaluation indices for the cell viability that were independent of the cell size.

Introduction

Cell freezing is widely used in regenerative medicine and cryosurgery, and it is important to prevent cell damage during cell freezing. Studies have indicated that in addition to osmotic stress, cell damage at low cooling rates is due to cell compression caused by the development of ice crystals that form outside the cells [2-6]. Cells appear to be compressed in the narrow spaces between the many needle-shaped ice crystals that develop [7,8]. Therefore, the damage mechanism is thought to be the mechanical stress of compressive deformation causing cells to break down, leading to lysis. This compression can be modeled as the compression of two parallel plates on a single cell. Takamatsu, et al. [1,9] performed compression experiments by placing a cell between two parallel plates and investigated the relationship between the reduction rate of the gap between the plates and the cell viability. There have been extensive studies for deriving the mechanical properties of cells from their responses when subjected to mechanical stress [10-14]. The measurement of the mechanical properties of cells allows the mechanical modeling of the deformation of the cell membrane and cytoskeleton, and the relationships between the changes in mechanical properties and the lesion state of the cell can be investigated. In experiments where cells were compressed by parallel plates, the relationship between the force and displacement

or between the stress and strain has been determined using microcantilevers [15-18].

In the present study, the compressive deformation of cells was analyzed using a method wherein microcapsules were compressively deformed by parallel plates [19]. The target cells were human prostatic adenocarcinoma cells, which had previously been subjected to plate compression experiments and their viability was measured [1]. We performed calculations corresponding to this experiment to determine the cell strain, the tension generated in the membrane, and the pressure difference between the inside and outside of the cell for the compressive force. When cells are compressed, the membrane undergoes expansion strain and shear strain, but it is shown that the expansion tension is related to cell lysis, and a relationship between the maximum value of the expansion tension and the cell viability is determined. During cell freezing, the osmotic pressure of the surrounding solution changes, along with the cell size. The surface area increases when the cells are compressed, and the relationship between the rate of increase of the surface area and the cell lysis is investigated. We show that the evaluation indices for the cell viability that are independent of the cell size are the rate of increase of the surface area and the deformation shape of the cell.

Analysis

A computational model of a spherical cell compressed by two parallel plates is shown in Figure 1. The deformation is assumed to be axisymmetric, and only the upper half is treated assuming the vertical symmetry of the shape. The initial radius of the cell is denoted as R_i, and the displacement of the upper half when it is compressed by the plate is denoted as δ. The cytoskeleton consists of actin filaments, microtubules, and intermediate filaments. The actin filaments, which exist along the inner side of the cell membrane, mainly support the mechanical structure of the surface [20]. Therefore, we modeled the cell surface as an elastic membrane. In addition, the actin filaments, microtubules, and intermediate filaments inside the cell support the structure of the whole cell [17]. Therefore, we represent the actions of these components as the maintenance of the original volume of the whole cell. Cells adhere to the plates during plate compression, and in general, membrane tension is generated when cells adhere to a plate [21,22]. This tension is treated as the initial tension and modeled as follows. When there is no tension in the cell membrane, the cell is a sphere of radius R_0, and the initial tension T_i is generated when the sphere expands to radius R_i. At this time, the initial stretch of the membrane is $\lambda_i = R_i / R_0$. The axis along the meridian of the sphere of radius R_0 is denoted as S, and that along the meridian of the shape after deformation due to plate compression is denoted as s. The angle between axis s and axis r is denoted as ψ. For an axisymmetric elastic membrane, the equations of the static force balance in the tangential and normal directions in the meridian plane are given as follows [10], in which the bending stiffness of the membrane is ignored.

$$\frac{dT_s}{ds} + \frac{1}{r}\frac{dr}{ds}(T_s - T_\varphi) = 0$$

$$\kappa_s T_s + \kappa_\varphi T_\varphi = p_{tr}$$

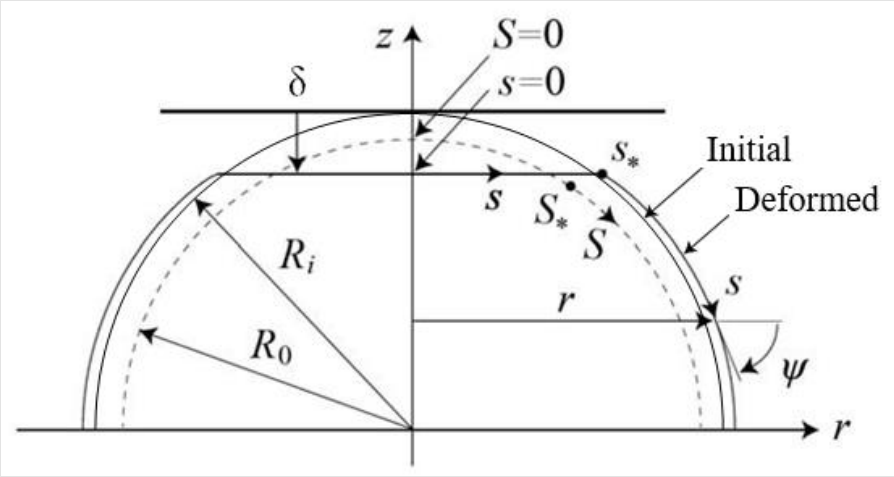

Figure 1: Analysis model.

Here, T_s and T_φ represent the principal tensions in the meridian plane and the principal tension in the circumferential direction, respectively. κ_s and κ_φ represent the principal curvature in the meridian plane and the principal curvature in the orthogonal plane, respectively. p_{tr} represents the transmural pressure, i.e., the pressure difference between the inside and outside (internal pressure – external pressure). The principal stretch in the meridian plane λ_s and the circumferential principal stretch λ_φ are given by $\lambda_s = ds/dS$, $\lambda_\varphi = r/R$, where R represents the r coordinate in the initial state of the material point after deformation. The tensions T_s and T_φ are calculated using Evans and Skalak's model [10] for biological membranes;

$T_s = K(\lambda_s\lambda_\varphi - 1) + \mu(\lambda_s^2 - \lambda_\varphi^2)/2\lambda_s^2\lambda_\varphi^2$, and T_φ is obtained by interchanging λ_s and λ_φ in T_s.

$K(= Eh/2(1-\nu))$ represents the area-expansion modulus, and $\mu(= Eh/2(1+\nu))$ represents the shear modulus. Here, E represents the Young's modulus, h the membrane thickness, and ν the Poisson's ratio. The isotropic tensions, i.e., the expansion tension T_e, the shear tension T_{sh}, and the Mises tension T_M, which is used to predict material failure according to the yield condition of the material, are determined using the following equations.

$$T_e = (T_s + T_\varphi)/2,\ T_{sh} = |T_s - T_\varphi|/2,\ T_M = \sqrt{T_s^2 + T_\varphi^2 - T_sT_\varphi}$$

The Young's modulus E and Poisson's ratio ν are for membranes, but when determining the elastic modulus of a cell using atomic force microscopy, the Young's modulus E' of the entire cell is often determined using the relationship between the force and displacement for the entire cell. Therefore, the approximate relationship $Eh = E'R_i$ for ν = 0.5 was used to obtain the Eh from E' and R_i. The above equations were solved under the condition that the volume inside the cell does not change and the symmetry conditions of the shape at z = 0 (i.e.ψ = π /2) to determine the strain of the cell, deformation shape, tension distribution, and pressure difference for the compressive force. The calculation method was described in detail in [19].

Results and Discussion

To validate the computational model, a comparison with experimental results (16) was performed. In this experiment, a single endothelial cell was subjected to a compression test using parallel plates, and the relationship between the force F and the compressive strain ε (= δ / R_i) was determined, as shown in Figure 2. In the calculation, the cell diameter was assumed to be 17.4μm, according to the experimental images. The Young's modulus E' of the whole cell was set as 1220Pa according to the Young's modulus of the cytoplasm (1000Pa), the Young's modulus of the nucleus (2500Pa), and the estimated volume ratio of the nucleus to the cytoplasm (0.17). Fitting to the experimental results was performed with the initial stretch set as λ_i = 1.12. The calculation results are indicated by the solid line in Figure 2. They agreed well with the experimental results with reasonable errors. According to the calculation, the initial tension determined from the initial stretch of the membrane was 2.7mN/m. According to measurements of HeLa cells (15-25μm in diameter) attached to a substrate, the membrane tension ranged from 2.73 to 3.62mN/m [22]. The results of the present calculations are close to these values.

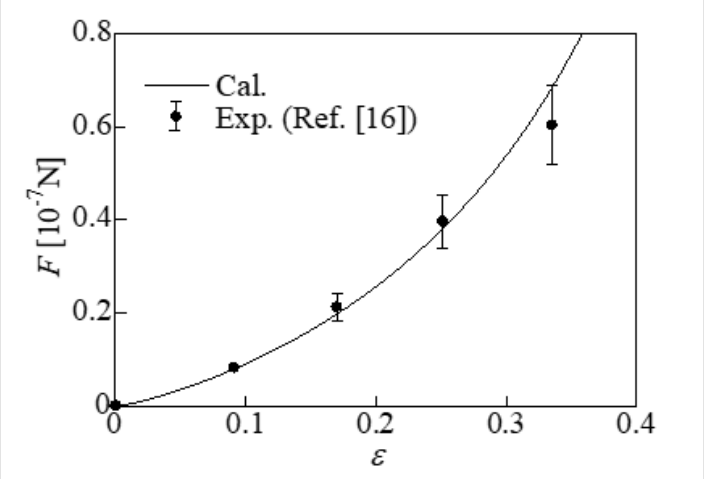

Figure 2: Relationship between the force and compressive strain.

When cells are frozen at a low temperature drop rate, ice crystals develop in a needle-like shape on the outside of the cells over time, and the cells appear to be compressed in the narrow spaces between the crystals [7,8]. Therefore, Takamatsu, et al. [1] hypothesized that the mechanical stress of compression is a major cause of cell damage during cell freezing, and as a model experiment, they performed compression tests on cells using parallel plates and investigated the relationship between the compression rate and the

cell viability. The target cells were human prostatic adenocarcinoma cells. In the experiment, the change in the cell size caused by the change in the external osmotic pressure generated during cell freezing was considered; i.e., compression testing was performed on these cells by changing the concentration of an extracellular NaCl aqueous solution, which changed the cell diameter to 15.4, 17.8, and 20.5μm. Table 1 presents the relationship between the compressive strain ε and the cell viability, which were averaged for the three kind of cells. The data were taken from Figure 6 in Ref. [1]. For the cell with diameter d (= $2R_i$) = 17.8μm, calculations were performed for compression due to parallel plates. The Young's modulus of the membrane E of prostate cancer was calculated using the measured Young's modulus of a whole cell, i.e., E' = 452Pa [23]. The initial stretch was set as λ_i = 1.12, which was used in the calculation shown in Figure 2. The calculation results for the relationship between the compressive force F and the strain ε are presented in Figure 3. When the strain was larger than ε = 0.7, the force F increased rapidly; thus, the viability decreased significantly, as shown in Table 1.

Table 1: Relationship between the compressive strain and the cell viability [1].

ε [-]	0.47	0.6	0.69	0.75	0.81
Viability [%]	80	65	50	35	20

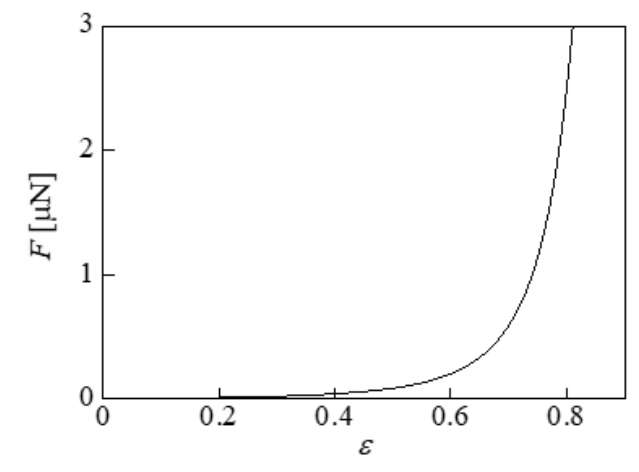

Figure 3: Relationship between the compressive force and the strain (d = 17.8μm).

Figure 4 shows the variations in the expansion tension T_e and shear tension T_{sh} with respect to the dimensionless S' $(= 2S/\pi R_0)$ when the strain ε was varied. The white circles in the figure indicate the points corresponding to S_*. The contact area with the plate is shown on the left of the white circles, and the non-contact area with the plate is shown on the right. T_e was approximately uniform on the membrane and was maximized at S' = 1 ; i.e., at z = 0. In addition, T_e increased with the strain ε. The shear tension T_{sh} increased with S' and was maximized at z = 0. However, T_{sh} was approximately one order of magnitude lower than T_e. Figure 5 shows that the distribution of the Mises tension T_M was almost identical to T_e in Figure 4, indicating that the expansion tension caused cell lysis.

Figure 6 shows the relationship between the strain and the pressure difference. When a cell lyses, the pressure difference is thought to decrease to zero from the pressure difference immediately before the lysis. The volume loss during compression is derived from $dV = AL_p p_{tr} dt$, where L_p is the water permeability of the cell membrane. The value for the erythrocyte membrane $L_p = 0.92 \times 10^{-12}$m/sPa [24] was used as L_p, the surface area of a spherical cell of diameter 17.8μm was used as the surface area A, and dt represents the time (10min) that the cell was under compression [1]. The rates of volume loss were 19% and 37% at p_{tr} = 1 and 2 kPa, respectively. In this cell model, the cytoskeleton inside the cell works to keep the volume of the whole cell constant, and the water permeability of the membrane is ignored.

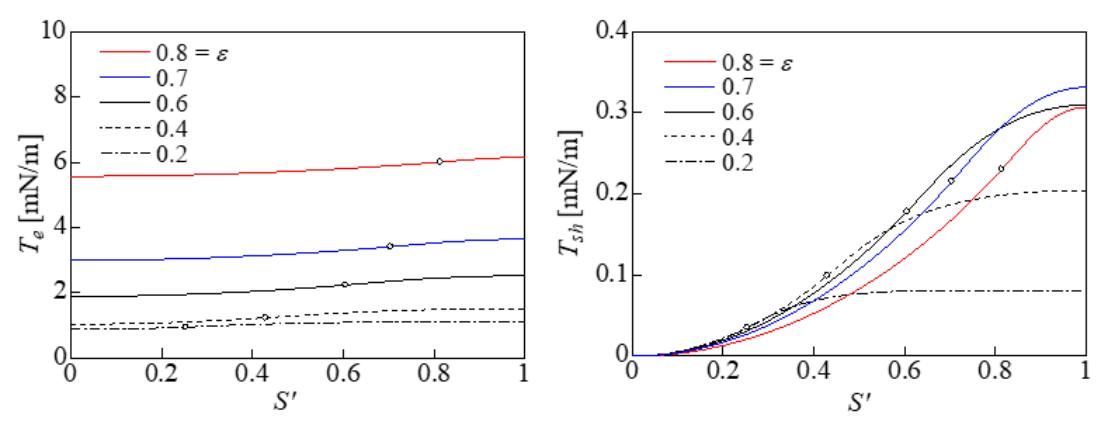

Figure 4: Variations in T_e and T_{sh} (d = 17.8μm).

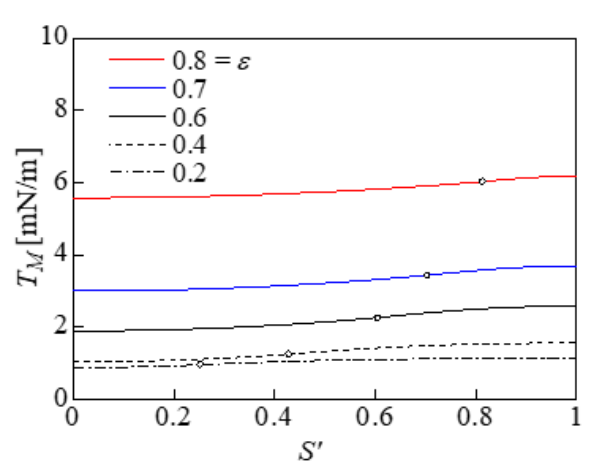

Figure 5: Variations in T_M (d = 17.8μm).

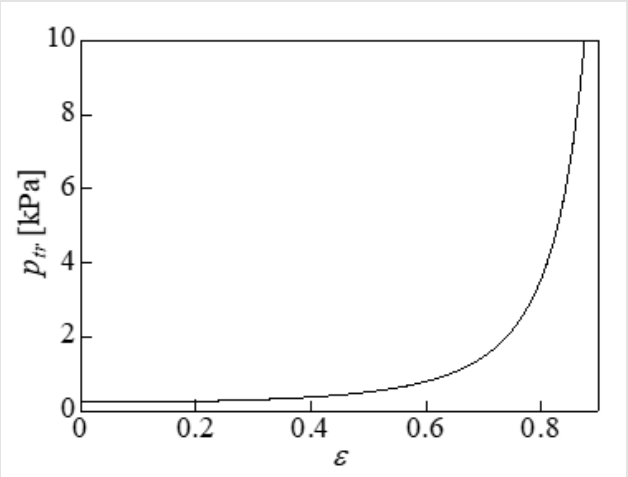

Figure 6: Relationship between the pressure difference and the strain (d = 17.8μm).

To investigate the effect of the change in the cell diameter on the tension, we performed calculations for cells with diameters of 15.4, 17.8, and 20.5μm with ε = 0.7 and 0.8. The calculation results for T_e and T_{sh} are shown in Figure 7. T_e and T_{sh} both increased with the diameter. Therefore, it was expected that a larger diameter would correspond to lower cell viability, similar to the results of a

previous experiment [1]. Figure 8 shows the relationship between the maximum value of T_e, i.e., $T_{e,max}$, and the viability of cells with a diameter of 17.8μm. The error bars in Figure 8 indicate the changes in $T_{e,max}$ when the diameter changed from 15.4 to 20.5μm. The causal factor triggering the cell lysis was thought to be the $T_{e,max}$ in Figure 8. The positions of $T_{e,max}$ are indicated by the black dots in Figure 11. The cytoskeletal structure of erythrocytes is mainly composed of spectrin on the inner side of the cell membrane, which differs from the cytoskeletal structure of prostatic adenocarcinoma cells. The expansion tension at which erythrocytes undergo hemolysis is T_h = 15mN/m [25], which exceeds the maximum value ($T_{e,max}$) in Figure 8. The radius of the erythrocyte when it was expanded to a sphere without changing the surface area from its initial value of 138μm^2 [26] was assumed to be r_h. The pressure difference p_{tr} at this time was p_{tr} = 9.1 kPa calculated by the Laplace equation $p_{tr} = 2T_h / r_h$. This was the pressure difference that causes hemolysis of erythrocytes. By comparing this value with the results shown in Figure 6, the compressive strain was determined to be 0. 87.

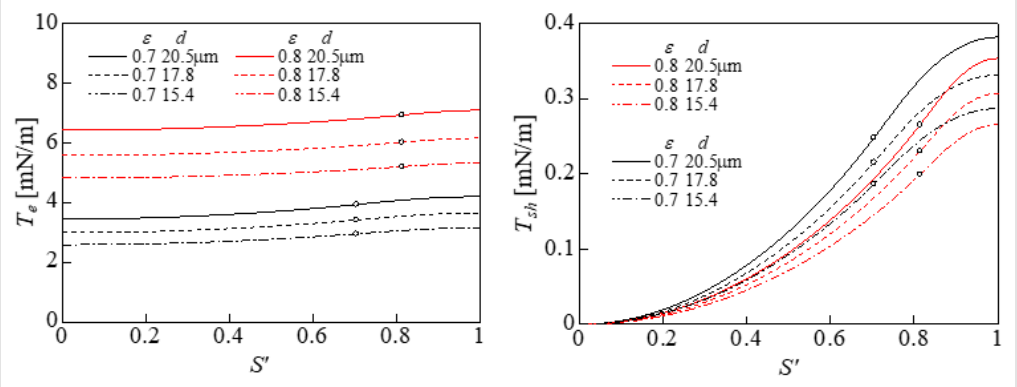

Figure 7: Changes in T_e and T_{sh}.

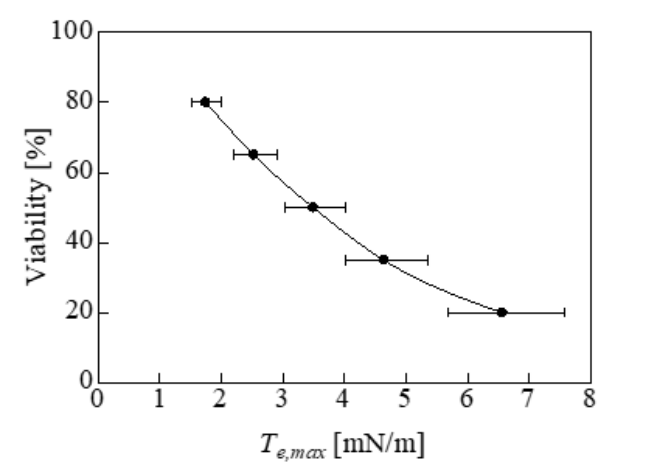

Figure 8: Relationship between the maximum expansion tension and the cell viability.

The surface area increases when cells are compressed. The results of the effect of the change in the cell diameter on the rate of increase of the surface area A/A_i during compression are presented in Figure 9. Here, $A_i(=\pi d^2/2)$ represents the surface area in the initial state. As shown in Figure 9, the effect of the change in the cell diameter on A/A_i was negligible. Therefore, the rate of increase of the surface area was independent of the cell size and was used as an evaluation index for the cell viability. Figure 10 shows the relationship between A/A_i and the viability. The results shown in Figures 9 & 10 are almost the same as those in Ref. [1]. Figure 11 shows the deformed shape of the cell resulting from compression. Here, ε = 0, 0.47, 0.69 and 0.81 correspond to the initial state and the compression states at 80%, 50%, and 20% viability, respectively. Because the deformation shape was independent of the cell diameter, a dimensionless representation with the initial radius R_i as the representative length is presented in Figure 11. Thus, the deformation shape was independent of the cell size and was used as an evaluation index for the cell viability. The black circle indicates the position where the expansion tension reached its maximum value $T_{e,max}$.

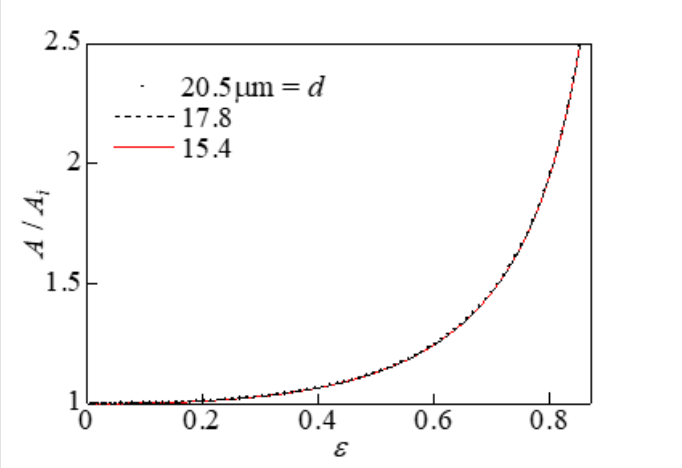

Figure 9: Relationship between the strain and the rate of increase of the surface area.

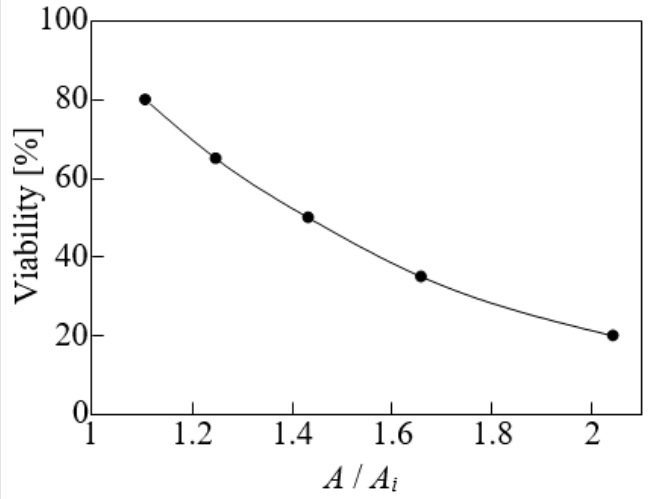

Figure 10: Relationship between the rate of increase of the surface area and the cell viability.

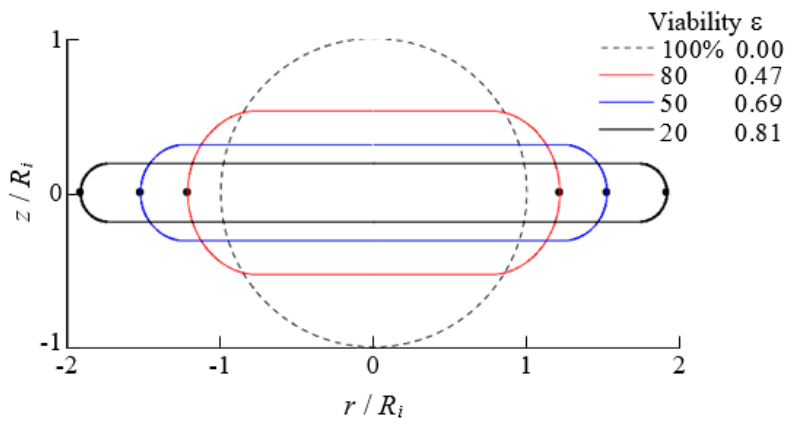

Figure 11: Relationship between the dimensionless deformation shape resulting from compression and the cell viability.

Conclusion

We performed calculations to model the process of cells being compressed by the development of external ice crystals in cell freezing under a slow temperature drop and obtained the following results.

1) The cause of cell lysis was expansion tension in the membrane of cortical actin filaments, and the effect of shear tension was negligible.

2) When the cell size increased owing to external osmotic pressure, the expansion tension due to the compression increased. Therefore, larger cells had lower viability under compression.

3) For prostatic adenocarcinoma cells with a diameter of 17.8μm, the expansion tensions that resulted in 50% and 20% viability were 3.5 and 6.6mN/m, respectively, and the rates of increase in the surface area were 1.4 and 2.0, respectively.

4) The rate of increase of the surface area under compression and the deformation shape are indices of the cell viability, because they are independent of the cell size in the range from d =15.4 to 20.5μm.

References

1. Takamatsu H, Takeya R, Naito S, Sumimoto H (2005) On the mechanism of cell lysis by deformation. Journal of Biomechanics 38(1): 117-124.
2. Maximov NA (1929) Internal factors of frost and drought resistance in plants. Protoplasma 7: 259-291.
3. Nei T (1967) Mechanism of hemolysis of erythrocytes by freezing at near-zero temperatures: I. Microscopic observation of hemolyzing erythrocytes during the freezing and thawing process. Cryobiology 4(3): 153-156.
4. Mazur P, Rall WF, Rigopoulos N (1981) Relative contributions of the fraction of unfrozen water and of salt concentration to the survival of slowly frozen human erythrocytes. Biophysical Journal 36(3): 653-675.
5. Rubinsky B (2000) Cryosurgery. Annual Review of Biomedical Engineering 2: 157-187.
6. Arora R (2018) Mechanism of freeze-thaw injury and recovery: A cool retrospective and warming up to new ideas. Plant Science 270: 301-313.
7. Ishiguro H, Rubinsky B (1994) Mechanical interactions between ice crystals and red blood cells during directional solidification. Cryobiology 31(5): 483-500.
8. Koushafar H, Rubinsky B (1997) Effect of antifreeze proteins on frozen primary prostatic adenocarcinoma cells. Urology 49(3): 421-425.
9. Takamatsu H, Kumagae N (2002) Survival of biological cells deformed in a narrow gap. Journal of Biomechanical Engineering 124(6): 780-783.
10. Evans EA, Skalak R (1980) Mechanics and thermodynamics of biomembranes. In: Evans EA, Skalak R (Eds.). CRC Press, Boca Raton USA.
11. Lim CT, Zhou EH, Quek ST (2006) Mechanical models for living cells - a review. Journal of Biomechanics 39(2): 195-216.
12. Suresh S (2007) Biomechanics and biophysics of cancer cells. Acta Biomaterialia 3(4): 413-438.
13. Kim DH, Wong PK, Park J, Levchenko A, Sun Y (2009) Microengineered platforms for cell mechanobiology, Annual Review of Biomedical Engineering 11: 203-233.
14. Unal M, Alapan Y, Jia H, Varga AG, Angelino K, et al. (2014) Micro and nano-scale technologies for cell mechanics. Nanobiomedicine 1: 29.
15. Thoumine O, Ott A (1997) Time scale dependent viscoelastic and contractile regimes in fibroblasts probed by microplate manipulation. Journal of Cell Science 110(17): 2109-2116.
16. Caille N, Thoumine O, Tardy Y, Meister JJ (2002) Contribution of the nucleus to the mechanical properties of endothelial cells. Journal of Biomechanics 35(2): 177-187.
17. Ofek G, Wiltz DC, Athanasiou KA (2009) Contribution of the cytoskeleton to the compressive properties and recovery behavior of single cells. Biophysical Journal 97(7): 1873-1882.
18. Wu TH, Chiou YW, Chiu WT, Tang MJ, Chen CH, et al. (2014) The F-actin and adherence-dependent mechanical differentiation of normal epithelial cells after TGF-β_1-induced EMT (tEMT) using a microplate measurement system. Biomedical Microdevices 16(3): 465-478.
19. Bando K (2013) Compressive deformation analysis of Alginate-Poly(L) lysine-Alginate (APA) microcapsule. Journal of Biomechanical Science and Engineering 8(1): 40-48.
20. Langelier E, Suetterlin R, Hoemann CD, Aebi U, Buschmann MD (2000) The chondrocyte cytoskeleton in mature articular cartilage: Structure and distribution of actin, tubulin, and vimentin filaments. Journal of Histochemistry & Cytochemistry 48(10): 1307-1320.
21. Pourati J, Maniotis A, Spiegel D, Schaffer JL, Bulter JP, et al. (1998) Is cytoskeletal tension a major determinant of cell deformability in adherent endothelial cells?. American Journal of Physiology 274(5): C1283-C1289.
22. Colbert MJ, Raegen AN, Fradin C, Dalnoki Veress K (2009) Adhesion and membrane tension of single vesicles and living cells using a micropipette-based technique. European Physical Journal E 30(2): 117-121.
23. Zouaoui J, Trunfio Sfarghiu AM, Brizuela L, Piednoir A, Maniti O, et al. (2017) Multi-scale mechanical characterization of prostate cancer cell lines: Relevant biological markers to evaluate the cell metastatic potential. Biochimica et Biophysica Acta - General Subjects 1861: 3109-3119.
24. Katchalsky A, Curran PF (1975) Nonequilibrium thermodynamics in biophysics. Misuzu Shobo. Tokyo Japan.
25. Canham PB, Parkinson DR (1970) The area and volume of single human erythrocytes during gradual osmotic swelling to hemolysis. Canadian Journal of Physiology and Pharmacology 48: 369-376.
26. Burton AC (1972) Physiology and biophysics of the circulation; An introductory text (2nd Edn.)., In: Burton AC (Edt.)., Year Book Medical Publishers. Chicago USA.

ISSN: 2574-1241

DOI: 10.26717/BJSTR.2022.42.006716

Kiyoshi Bando. Biomed J Sci & Tech Res